1 and 2, CASSCF multiconfigurational calculations were performed with active spaces of three orbitals and two electrons. For the singly bridged structures 2, the corresponding multiconfigurational wave function involves four configurations. The energy lowering brought by the CASSCF procedure with respect to the SCF energy represents the intrapair correlation energy of the X-H-X two-electron bridge in 2. It is calculated at 16.3 kcal/mol in $C_2H_5^+$, 13.6 kcal/mol in $Si_2H_5^+$, and 14.4 kcal/mol in $Pb_2H_5^+$. Similar valence correlation energies were obtained in the corresponding neutral or dicationic singly or doubly bridged systems.[11,23] For the classical form 1 of $Si_2H_5^+$, such an active space keeps localized on the $Si_1$-$H_1$ region, and the CASSCF extra energy (12.1 kcal/mol) now corresponds to the correlation energy of this Si-H bond.

# Ab Initio Calculations on the Lower Excited States of Short-Chain Polyenals

**Marianne Ros,[†] Edgar J. J. Groenen,*[,†] and Marc C. van Hemert[‡]**

*Contribution from the Centre for the Study of Excited States of Molecules, Huygens Laboratory, P.O. Box 9504, and Department of Chemistry, Gorlaeus Laboratories, P.O. Box 9502, University of Leiden, 2300 RA Leiden, The Netherlands.* *Received January 21, 1992*

**Abstract:** The lower excited states of the planar all-trans isomers of crotonaldehyde, hexadienal, and octatrienal have been investigated by multi-reference single and double excitation configuration interaction (MRD-CI) calculations. For crotonaldehyde we find both the lowest excited singlet state $S_1$ and the lowest triplet state $T_0$ to be $n\pi^*$ in nature; for hexadienal and octatrienal $S_1$ is $n\pi^*$ and $T_0$ is $\pi\pi^*$ in nature. Bond-order reversal stabilizes the lower excited states and destabilizes the ground state. The $\pi\pi^*$ states decrease more in energy than the $n\pi^*$ states upon lengthening the polyenal. We calculate the radiative lifetime of the $^3\pi\pi^*$ state in the ground-state geometry to vary from 35 ms for crotonaldehyde to 75 s for octatrienal and explain the absence of phosphorescence for polyenals.

## 1. Introduction

The low-lying excited states of linear conjugated molecules continue to attract attention from spectroscopists and theoreticians because of the role played by such compounds in photochemical processes as photoisomerization and photoconductivity. These chromophores are much more difficult to understand than one would judge from their simple composition, and even the quantum-chemical description of relatively short chains presents significant problems. Here we report on ab initio calculations for three polyenals $CH_3(—CH=CH)_n—CHO$: *trans*-crotonaldehyde (CA, $n = 1$), *all-trans*-hexadienal (HD, $n = 2$), and *all-trans*-octatrienal (OT, $n = 3$).

Experimental observations on polyenals largely concern their excited singlet states. Birge et al. studied the vapor-phase absorption spectra for CA in the wavelength region corresponding to the excitation into the first $^1n\pi^*$ state.[1] These authors concluded that in this state CA is approximately planar and that considerable bond-order reversal takes place, i.e. double bonds become longer and single bonds become shorter upon excitation. Das and Becker recorded absorption and emission spectra for a series of unsubstituted polyenals in order to determine the singlet-state ordering as a function of chain length.[2] For $n \leq 3$ they concluded the lowest excited singlet state to be $n\pi^*$ in nature.

Polyenals do not phosphoresce, which severely hinders the investigation of their lowest triplet state. From singlet-triplet absorption spectra Birge et al. assigned for CA the lowest triplet state to be of $n\pi^*$ character.[3] These authors asserted that, as for the $^1n\pi^*$ state, CA in the $^3n\pi^*$ state is planar and the bond orders are reversed. On the other hand, from time-resolved EPR spectra Yamauchi et al.[4] claimed the relaxed lowest triplet state of CA to be of $\pi\pi^*$ character and the molecule to twist severely about the ethylenic bond upon triplet excitation. Evans determined the location of the lowest triplet state of polyenals with $n = 3$, 4, and 5 by recording $S_0 \rightarrow T_0$ absorption spectra in the presence of high-pressure oxygen.[5] Recently, Ros et al. identified by electron-spin-echo (ESE) spectroscopy the lowest triplet state of polyenals with $n = 2$, 3, 4, and 5 as a $\pi\pi^*$ state and concluded that these molecules are planar in $T_0$.[6]

Theoretical chemical studies of polyenals are scarce. To the best of our knowledge calculations of all-trans isomers of polyenals have not been carried out with ab initio methods so far. For CA Birge et al.[3] and Boerth[7] performed CNDO/II and INDOUV calculations, respectively, in order to determine the energy of the lower excited singlet and triplet states. For polyenals that lack the terminal methyl group Inuzuka and Becker calculated excited-state energies within the framework of PPP-SCF-MO-CI.[8] They found the lowest triplet state for $n > 1$ to be $\pi\pi^*$ and the lowest excited singlet state for $n < 4$ to be $n\pi^*$. According to their calculations the energy of the $n\pi^*$ states remained constant and that of the $\pi\pi^*$ states decreased upon increasing the chain length.

As far as $\pi\pi^*$ states are concerned we can relate the description of polyenals to that of polyenes, linear conjugated chains without the aldehyde group. Lack of intersystem crossing for polyenes has severely precluded the investigation of their triplet-state properties. Regarding the singlets, a major advance in understanding was made by the discovery of a low-lying excited singlet state of $A_g$ character, to which the transition from $S_0$ is electric-dipole forbidden.[9] An adequate theoretical description of this state requires a proper inclusion of electron correlation. The singlet-state ordering is only correctly reproduced by a configu-

[†] Huygens Laboratory.
[‡] Gorlaeus Laboratories.

(1) Birge, R. R.; Pringle, W. C.; Leermakers, P. A. *J. Am. Chem. Soc.* **1971**, *93*, 6715.
(2) Das, P. K.; Becker, R. S. *J. Phys. Chem.* **1982**, *86*, 921.
(3) Birge, R. R.; Leermakers, P. A. *J. Am. Chem. Soc.* **1972**, *94*, 8105.
(4) Yamauchi, S.; Hirota, N.; Higuchi, J. *J. Phys. Chem.* **1988**, *92*, 2129.
(5) Evans, D. F. *J. Chem. Soc.* **1960**, 1735.
(6) Ros, M.; Groenen, E. J. J. *Chem. Phys. Lett.* **1989**, *154*, 29. Ros, M.; Groenen, E. J. J. *J. Chem. Phys.* **1991**, *94*, 7640.
(7) Boerth, D. W. *J. Org. Chem.* **1982**, *47*, 4085.
(8) Inuzuka, K.; Becker, R. S. *Bull. Chem. Soc. Jpn.* **1972**, *45*, 1557. Inuzuka, K.; Becker, R. S. *Bull. Chem. Soc. Jpn.* **1974**, *47*, 88.
(9) Hudson, B. S.; Kohler, B. E.; Schulten, K. In *Excited States*; Lim, E. C., Ed.; Academic Press: New York, 1982; Vol. 6, p 1.

0002-7863/92/1514-6820$03.00/0 

**Table I.** Details of the CI Calculations Carried Out for Crotonaldehyde in the G, I, and E Geometries[a]

| state | dominant reference config | contribution in CI: $c^2$ (%)/$\sum_i c_i^2$ (%) | | | energy (hartree) | | |
|---|---|---|---|---|---|---|---|
| | | G | I | E | G | I | E |
| $1^1A'$ ($S_0$) | ground state | 89/92 | 88/92 | 87/92 | -230.0006 | -230.0019 | -229.9865 |
| $2^1A'$ ($^1B_u^*$) | $\pi_3 \rightarrow \pi_4^*$ | 85/90 | 85/90 | 72/90 | -229.7585 | -229.7619 | -229.7758 |
| $3^1A'$ ($^1A_g^*$) | $\pi_3 \rightarrow \pi_5^*$ | 40/91 | 26/93 | 25/91 | -229.6999 | -229.7596 | -229.7598 |
| | $\pi_2 \rightarrow \pi_4^*$ | 16 | 23 | 19 | | | |
| | $\pi_3,\pi_3 \rightarrow \pi_4^*,\pi_4^*$ | 14 | 21 | 18 | | | |
| $1^1A''$ ($^1n\pi^*$) | $n \rightarrow \pi_4^*$ | 72/91 | 72/91 | 71/91 | -229.8510 | -229.8696 | -229.8803 |
| $2^1A''$ | $n \rightarrow \pi_5^*$ | 56/89 | 54/90 | 53/90 | -229.7397 | -229.7598 | -229.7578 |
| | $n, \pi_3 \rightarrow \pi_4^*,\pi_4^*$ | 17 | 19 | 17 | | | |
| $1^3A'$ ($^3\pi\pi^*$) | $\pi_3 \rightarrow \pi_4^*$ | 85/94 | 86/94 | 86/93 | -229.8570 | -229.8857 | -229.8920 |
| $2^3A'$ | $\pi_2 \rightarrow \pi_4^*$ | 48/94 | 49/94 | 52/91 | -229.7735 | -229.7948 | -229.7920 |
| | $\pi_3 \rightarrow \pi_5^*$ | 29 | 31 | 29 | | | |
| $1^3A''$ ($^3n\pi^*$) | $n \rightarrow \pi_4^*$ | 72/92 | 73/92 | 73/92 | -229.8617 | -229.8758 | -229.8852 |
| | $n \rightarrow \pi_5^*$ | 12 | 9 | 6 | | | |
| $2^3A''$ | $n \rightarrow \pi_5^*$ | 51/90 | 49/91 | 48/90 | -229.7451 | -229.7578 | -229.7583 |
| | $n,\pi_3 \rightarrow \pi_4^*,\pi_4^*$ | 19 | 21 | 21 | | | |

[a] In the first column the labels between parentheses refer to spectroscopic usage; in the third column $c^2$ is the square of the coefficient of the configuration in the second column in the final CI wave function and $\sum_i c_i^2$ is the sum of the squared contributions of the reference configurations; 1 hartree = 27.211 eV. In the second column only those configurations are shown for which $c^2$ is at least 10% for one of the geometries.

ration-interaction (CI) treatment that takes into account doubly excited configurations.[10] For polyenes larger than butadiene this $2^1A_g$ state was found to be the lowest excited singlet state.[11] The state observed in absorption is of $B_u$ character and can be represented simply by a promotion of one electron from the highest occupied $\pi$-orbital to the lowest unoccupied $\pi^*$-orbital.

Here we present an ab initio study of the unsubstituted polyenals CA, HD, and OT and compare the results with spectroscopic observations. As far as we know these calculations are the first for CA that are carried out at the ab initio CI level and the very first for HD and OT. We adopt a planar geometry and calculate the wave functions and energies of the low-lying excited states. For $n$ = 1, 2, and 3 the lowest excited singlet state is found to be of $n\pi^*$ character and for $n > 1$ the lowest triplet state is of $\pi\pi^*$ character. On increasing the chain length the $\pi\pi^*$ states lower more in energy than the $n\pi^*$ states. Bond-order reversal stabilizes the excited states and destabilizes the ground state. Analysis of the spin–orbit coupling between the lowest $^1n\pi^*$ and $^3\pi\pi^*$ states and between the lowest $^3n\pi^*$ state and the ground state shows that the radiative lifetime for polyenals with $n$ = 1, 2, and 3 increases drastically with increasing chain length. The combination of these calculated radiative lifetimes with the experimental observations on the magnitude of and the trend in the non-radiative lifetime for polyenals with $n$ = 3, 4, and 5[6] enables us to explain the lack of phosphorescence for polyenals.

## 2. Computational Details

The calculations for the trans isomers of the polyenals ($n$ = 1, 2, and 3) started from a planar molecule because of the experimental evidence that neither in the ground state[12] nor in the $n\pi^*$ excited states[1,3,13] nor for $n \geq 2$ in the lowest triplet state[6] do polyenals undergo an out-of-plane distortion. Consequently, the compounds under consideration belong to the $C_{1h}$ group and the atomic orbitals, molecular orbitals, and electronic states can be classified according to the A′ and A″ irreducible representations of this point group. Within the restriction of planarity we considered different geometries. The first, henceforth denoted by G, concerned the structure of the ground state:[7] $r$(C=O) = 1.22 Å, $r$(C=C) = 1.34 Å, and $r$(C—C) = 1.46 Å. The second, henceforth denoted by E, concerned the structure for which the bond order is reversed with respect to the ground state:[14] $r$(C=O) = 1.32 Å, $r$(C=C) = 1.46 Å, and $r$(C—C) = 1.35 Å. Finally, for CA ($n$ = 1) we considered an additional intermediate (I) geometry, for which all bond lengths are the average of those employed in the G and the E geometries: $r$(C=O) = 1.27 Å, $r$(C=C) = 1.40 Å, and $r$(C—C) = 1.405 Å. For all calculations we took the distance between the methyl carbon and the adjacent carbon to be 1.52 Å, the distance between the methyl protons and the methyl carbon to be 1.09 Å, and the mutual distance between the protons and carbons along the chain to be 1.08 Å. The methyl group was positioned such that $C_{1h}$ symmetry was conserved and that the in-plane C—H bond was s-trans with the C=C bond. All bond angles adhered to strict tetragonal or trigonal values. In the remaining part of this section we present the computational details for CA with those for HD and OT enclosed in parentheses, i.e. in the form CA (HD, OT).

For the oxygen and carbon atoms we chose as an atomic orbital (AO) basis set the [4s 2p] Dunning contraction of the Huzinaga (9s 5p) Cartesian Gaussian set and for hydrogen the [2s] contraction of the (4s) set.[15] The total basis set therefore amounted to 62 (86, 110) AOs. For all geometries we calculated the ground-state SCF orbitals. We obtained an SCF ground-state energy of -229.7169 hartrees (-306.5747 hartrees, -383.4330 hartrees) for the G geometry and -229.6840 hartrees (-306.5272 hartrees, -383.3728 hartrees) for the E geometry. For the CI calculations we truncated the molecular orbital (MO) set to 47 (58, 72) MOs by freezing the 10 (16, 22) lower and 5 (12, 16) upper $\sigma$-type MOs of a′ symmetry. Consequently, a total number of 18 (20, 22) electrons were correlated.

We performed the CI calculations with the multi-reference single and double excitation CI method (MRD-CI) with configuration selection and energy extrapolation to the general MRD-CI space.[16] An estimate of the energy corresponding to the full CI space within the present AO basis set was made according to ref 17. The reference configurations in the CI were allowed to contain up to and including four open shells. The contribution of configurations with four open shells is especially critical for the description of A″ excited states and becomes more important the larger the molecule. In the CI we selected those reference configurations for which the magnitude of the coefficient in the CI expansion is larger than 0.05. This led to a set of about 30 (30, 40) reference configurations. From these typically 2 000 000 (4 000 000, 9 000 000) symmetry-adapted functions were generated for singlet states and about twice as many for triplet states. We used a configuration selection threshold of 15 $\mu$hartrees (12 $\mu$hartrees, 12 $\mu$hartrees), which for all molecules led to the inclusion of 5000–10000 symmetry-adapted functions in the secular equation that was eventually solved. The extrapolation uncertainty in the CI typically amounted to 0.003 hartree (0.004 hartree, 0.005 hartree) for the ground state and 0.006 hartree (0.007 hartree, 0.009 hartree) for excited states.

## 3. Results

**1. Wave Functions and Energies.** In Tables I–III we present the results of the CI calculations for the lower electronic states of CA, HD, and OT, respectively. In order to facilitate the description of the dominant configurations in the CI procedure, we name the MOs involved. From symmetry considerations the a″ MOs are $\pi$-orbitals. We indicate the three highest occupied MOs of this symmetry, ranked in order of increasing energy, with

(10) Schulten, K.; Karplus, M. *Chem. Phys. Lett.* **1972**, *14*, 305.
(11) Buma, W. J.; Kohler, B. E.; Song, K. *J. Chem. Phys.* **1990**, *92*, 4622.
(12) Suzuki, M.; Kozuma, K. *Bull. Chem. Soc. Jpn.* **1969**, *42*, 2183.
(13) Brand, J. C. D.; Williamson, D. G. *Discuss. Faraday Soc.* **1963**, *35*, 184.
(14) Hollas, J. M. *Spectrochim. Acta* **1963**, *19*, 1425.
(15) Dunning, Th., Jr. *J. Chem. Phys.* **1970**, *53*, 2823. Dunning, Th., Jr. *J. Chem. Phys.* **1971**, *55*, 716.
(16) Buenker, R. J.; Peyerimhoff, S. D.; Butscher, W. *Mol. Phys.* **1978**, *35*, 771.
(17) Bruna, P. J.; Peyerimhoff, S. D.; Buenker, R. J. *Chem. Phys. Lett.* **1980**, *72*, 278.

Table II. Details of the CI Calculations Carried Out for Hexadienal in the G and E Geometries[a]

| state | dominant reference config | contribution in CI: $c^2$ (%)/ $\sum_i c_i^2$ (%) G | E | energy (hartree) G | E |
|---|---|---|---|---|---|
| $1^1A'$ ($S_0$) | ground state | 87/91 | 82/91 | -306.8573 | -306.8345 |
| $2^1A'$ ($^1B_u^*$) | $\pi_3 \rightarrow \pi_4^*$ | 84/90 | 53/88 | -306.6397 | -306.6498 |
| $3^1A'$ ($^1A_g^*$) | $\pi_3 \rightarrow \pi_5^*$ | 27/88 | 28/89 | -306.6247 | -306.6989 |
| | $\pi_3,\pi_3 \rightarrow \pi_4^*,\pi_4^*$ | 24 | 28 | | |
| | $\pi_2 \rightarrow \pi_4^*$ | 18 | 12 | | |
| $1^1A''$ ($^1n\pi^*$) | $n \rightarrow \pi_4^*$ | 66/90 | 61/90 | -306.7034 | -306.7392 |
| $2^1A''$ | $n,\pi_3 \rightarrow \pi_4^*,\pi_4^*$ | 28/87 | 19/88 | -306.6157 | -306.6489 |
| | $n \rightarrow \pi_6^*$ | 27 | 17 | | |
| | $n \rightarrow \pi_5^*$ | 16 | 26 | | |
| $1^3A'$ ($^3\pi\pi^*$) | $\pi_3 \rightarrow \pi_4^*$ | 79/91 | 81/92 | -306.7440 | -306.7791 |
| $2^3A'$ | $\pi_2 \rightarrow \pi_4^*$ | 41/91 | 51/90 | -306.6865 | -306.6956 |
| | $\pi_3 \rightarrow \pi_5^*$ | 40 | 27 | | |
| $3^3A'$ | $\pi_1 \rightarrow \pi_4^*$ | 41/88 | 42/87 | -306.6494 | -306.6511 |
| $1^3A''$ ($^3n\pi^*$) | $n \rightarrow \pi_4^*$ | 65/91 | 62/90 | -306.7227 | -306.7474 |
| | $n,\pi_3 \rightarrow \pi_4^*,\pi_4^*$ | - | 12 | | |
| $2^3A''$ | $n,\pi_3 \rightarrow \pi_4^*,\pi_4^*$ | 30/88 | 22/89 | -306.6324 | -306.6702 |
| | $n \rightarrow \pi_6^*$ | 26 | 19 | | |
| | $n \rightarrow \pi_5^*$ | 13 | 23 | | |

[a] On going from G to E the $^1B_u^*$ and $^1A_g^*$ states cross, so for the E geometry the labels $2^1A'$ and $3^1A'$ should be interchanged. For further remarks see the caption of Table I.

Table III. Details of the CI Calculations Carried Out for Octatrienal in the G and E Geometries[a]

| state | dominant reference config | contribution in CI: $c^2$ (%)/ $\sum_i c_i^2$ (%) G | E | energy (hartree) G | E |
|---|---|---|---|---|---|
| $1^1A'$ ($S_0$) | ground state | 85/90 | 78/90 | -383.7362 | -383.7061 |
| $2^1A'$ ($^1B_u^*$) | $\pi_3 \rightarrow \pi_4^*$ | 71/89 | 63/88 | -383.5442 | -383.5575 |
| $3^1A'$ ($^1A_g^*$) | $\pi_3,\pi_3 \rightarrow \pi_4^*,\pi_4^*$ | 23/87 | 31/87 | -383.5328 | -383.6009 |
| | $\pi_2 \rightarrow \pi_4^*$ | 16 | 13 | | |
| | $\pi_3 \rightarrow \pi_5^*$ | 15 | 7 | | |
| | $\pi_3 \rightarrow \pi_4^*$ | 15 | 15 | | |
| $1^1A''$ ($^1n\pi^*$) | $n \rightarrow \pi_4^*$ | 58/89 | 53/89 | -383.5945 | -383.6382 |
| | $n \rightarrow \pi_5^*$ | 13 | - | | |
| | $n,\pi_3 \rightarrow \pi_4^*,\pi_4^*$ | - | 15 | | |
| $2^1A''$ | $n,\pi_3 \rightarrow \pi_4^*,\pi_4^*$ | 32/86 | 14/87 | -383.5247 | -383.5645 |
| | $n \rightarrow \pi_5^*$ | 17 | 32 | | |
| | $n \rightarrow \pi_7^*$ | 17 | 7 | | |
| | $n,\pi_2 \rightarrow \pi_4^*,\pi_4^*$ | - | 11 | | |
| $1^3A'$ ($^3\pi\pi^*$) | $\pi_3 \rightarrow \pi_4^*$ | 74/90 | 77/90 | -383.6539 | -383.6812 |
| $2^3A'$ | $\pi_2 \rightarrow \pi_4^*$ | 41/90 | 49/89 | -383.6149 | -383.6238 |
| | $\pi_3 \rightarrow \pi_5^*$ | 35 | 29 | | |
| $3^3A'$ | $\pi_3 \rightarrow \pi_6^*$ | 34/90 | 8/90 | -383.5946 | -383.6128 |
| | $\pi_1 \rightarrow \pi_4^*$ | 29 | 24 | | |
| | $\pi_2 \rightarrow \pi_5^*$ | 14 | - | | |
| | $\pi_3,\pi_3 \rightarrow \pi_4^*,\pi_5^*$ | - | 11 | | |
| | $\pi_2,\pi_3 \rightarrow \pi_4^*,\pi_4^*$ | - | 16 | | |
| $1^3A''$ ($^3n\pi^*$) | $n \rightarrow \pi_4^*$ | 57/89 | 54/90 | -383.6110 | -383.6525 |
| | $n \rightarrow \pi_5^*$ | 16 | - | | |
| | $n,\pi_3 \rightarrow \pi_4^*,\pi_4^*$ | - | 14 | | |
| $2^3A''$ | $n,\pi_3 \rightarrow \pi_4^*,\pi_4^*$ | 32/87 | 17/88 | -383.5358 | -383.5814 |
| | $n \rightarrow \pi_7^*$ | 18 | 8 | | |
| | $n \rightarrow \pi_5^*$ | 14 | 30 | | |

[a] On going from G to E the $^1B_u^*$ and $^1A_g^*$ states cross, so for the E geometry the labels $2^1A'$ and $3^1A'$ should be interchanged. For further remarks see the caption of Table I.

$\pi_1$, $\pi_2$, and $\pi_3$. Similarly, the lowest unoccupied a'' MOs are denoted by $\pi_4^*$, $\pi_5^*$, $\pi_6^*$, and $\pi_7^*$. The only MO of a' symmetry that plays a substantial part in the excitations considered is the highest occupied one indicated by n (cf. section 4.1). We first consider the results for CA in the G geometry and observe that the ground state ($1^1A'$) can almost be described by a single configuration. The lowest excited singlet state is of A'' character and represents the promotion of an electron from n to $\pi_4^*$. The second excited singlet state, A' in nature, concerns predominantly an excitation of a single electron from $\pi_3$ to $\pi_4^*$. To the following $^1A'$ excited state three configurations contribute significantly. One of these concerns a simultaneous excitation of two electrons, a so-called doubly excited configuration. As regards the triplet states, $1^3A''$ is lowest with $1^3A'$ lying close by. As is seen from Tables I–III bond-order reversal and lengthening of the chain affect the nature and the ordering of the lower excited states.

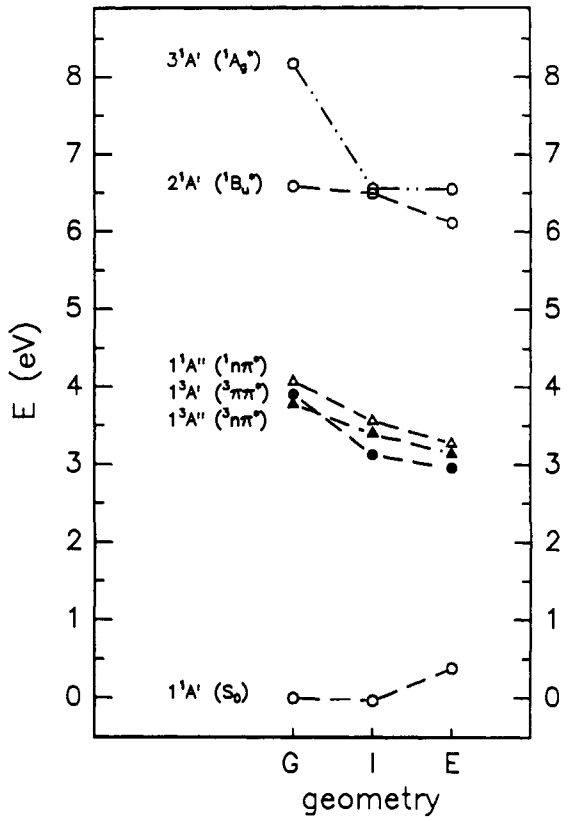


Figure 1. Plot of the energies of some lower electronic states for crotonaldehyde as a function of geometry: (○) $^1A'$, (△) $^1A''$, (●) $^3A'$, and (▲) $^3A''$ states. The $2^1A''$, $2^3A'$, and $2^3A''$ states are not reproduced in the figure. The zero of energy corresponds to the energy of the ground state in the G geometry.

In Figure 1 we visualize for CA the effect of a change in bond length on the energies of some selected electronic states: the ground state, the $1^1A''$, $1^3A'$, and $1^3A''$, and the $2^1A'$ and $3^1A'$ state. We observe that bond-order reversal raises the energy of the ground state and lowers that of the excited states. Evidence that for linear conjugated molecules such a geometry change may occur upon excitation is provided by time-resolved resonance Raman spectra of the lowest triplet state of hexatriene in combination with quantum-chemical force-field calculations.[18] The fall in energy on going from G to E as presently calculated is largest for the $3^1A'$ state (more than 1.5 eV) and smallest for the $2^1A'$ state (less than 0.5 eV). From Table I it is obvious that for the latter the $\pi_3 \rightarrow \pi_4^*$ configuration becomes less dominant. In Figure 1 it is seen that the $^3A'$ state is lowered more in energy than the $^3A''$ state and that the former becomes the lowest triplet state. As regards the results for the I geometry, we observe that, except for the ground state and the $2^3A'$ state (Table I), the energies are intermediate between the corresponding values for the G and the E geometry. For all excited states except the $2^1A'$ state the energy shift is largest in the G → I step.

With regard to the larger polyenals, mutual comparison of Tables I–III shows that a description of the electronic states in terms of one or two dominant configurations becomes less satisfactory. The influence of chain length on the excitation energy depends on the state considered and is visualized in Figure 2 for some selected electronic states for the G geometry and in Figure 3 for the E geometry. The increase in the number of double bonds hardly modifies the energy of the A'' states. On the other hand, the A' states are lowered in energy significantly. As a consequence,

(18) Negri, F.; Orlandi, G.; Brouwer, A. M.; Langkilde, F. W.; Wilbrandt, R. *J. Chem. Phys.* **1989**, *90*, 5944.

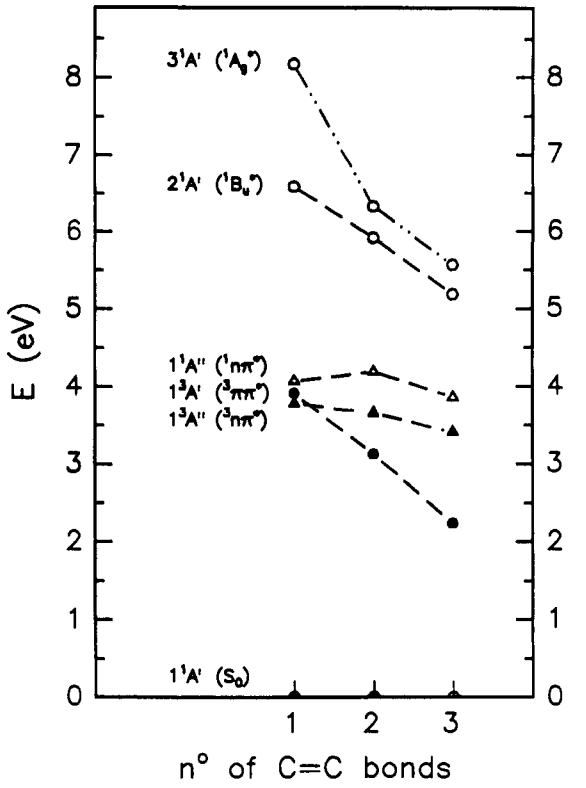


**Figure 2.** Plot of the effect of lengthening the chain on the excitation energies of some lower electronic states for the G geometry: (○) $^1A'$, (△) $^1A''$, (●) $^3A'$, and (▲) $^3A''$ states. The $2^1A''$, $2^3A'$, and $2^3A''$ states and the $3^3A'$ state are not reproduced in the figure. The zero of energy corresponds to the energy of the ground state in the G geometry.

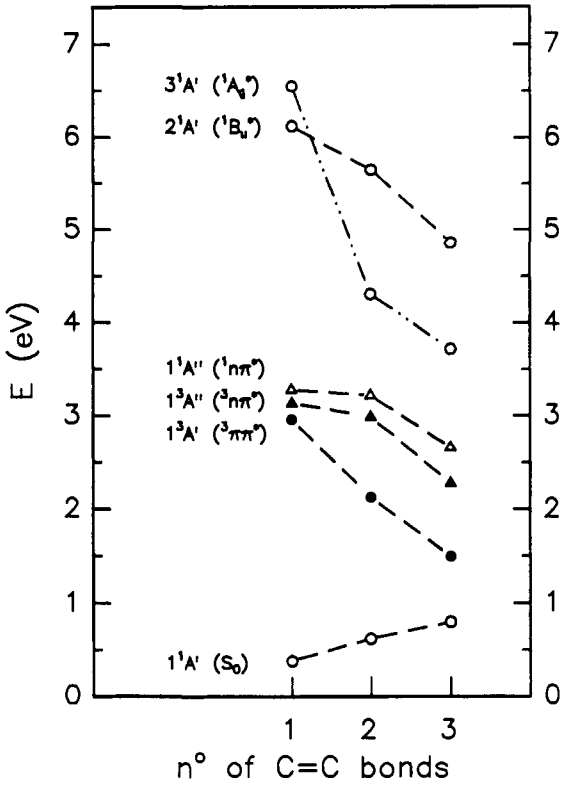


**Figure 3.** Plot of the effect of lengthening the chain on the excitation energies of some lower electronic states for the E geometry: (○) $^1A'$, (△) $^1A''$, (●) $^3A'$, and (▲) $^3A''$ states. The $2^1A''$, $2^3A'$, and $2^3A''$ states and the $3^3A'$ state are not reproduced in the figure. The zero of energy corresponds to the energy of the ground state in the G geometry.

for HD and OT the $1^3A'$ state is the lowest excited triplet state in the G geometry as well. The A′ state that stabilizes most is the $3^1A'$ state; for HD and OT the $2^1A'$ and $3^1A'$ levels cross upon relaxing from the G to the E geometry (cf. Figures 2 and 3). Figure 3 also demonstrates that the destabilization of the ground state in going from G to E increases upon lengthening the polyenal chain. In combination with the lowering of the $1^3A'$ level this results in a sharp reduction of the $S_0$–$T_0$ energy gap, which according to our calculations for OT merely amounts to 0.7 eV in the E geometry.

**2. Quality of the Calculations.** In performing the CI calculations for the polyenals a large number of reference configurations is needed to provide for an adequate description of the excited states. Moreover, in the CI for the A″ states, configurations that contain four open shells play a significant role. These facts may indicate that the MOs that are employed are not an entirely satisfactory starting point for the CI procedure. On the other hand, the quality of the calculations can be limited by the choice of the AO basis. In order to estimate the effect of these restrictions and the accuracy of the results presented in Tables I–III, we have performed additional MRD-CI calculations for CA in the G geometry, on the one hand starting from another MO set and on the other hand starting with an extended AO basis.

The CI results for excited states generally improve if an MO set consisting of excited-state SCF orbitals is employed. We carried out an SCF calculation on the $1^3A'$ state and used the resulting MOs as a starting point for the CI treatment. As expected the number of reference configurations needed in the CI of $^3A'$ states (and also slightly in that of the $^1A'$ states) decreases. However, we observe no significant changes in the nature and energies of the excited states as compared to the results calculated with ground-state SCF orbitals. The states are described by the same dominant configurations and the changes in excitation energies are less than ±0.25 eV. The ground state does not shift at all.

Extension of the AO basis set with diffuse orbitals has a much larger impact on the results. For CA we added Rydberg-type diffuse functions to oxygen and carbon. For oxygen we set the exponents of these single Gaussians at 0.032 and 0.028 for the s and p atomic orbitals respectively, for carbon at 0.023 and 0.020.[19] The total AO basis set consisted of 82 functions. For CA in the G geometry we calculated the ground-state SCF orbitals. CI calculations performed with these MOs still require about 30 reference configurations for a proper description of the excited states. Compared to the results of the standard CI treatment, discussed in section 3.1, we observe some significant differences. On addition of diffuse orbitals the $2^1A'$ state and the $1^3A'$ state acquire a substantial amount of diffuse character; in the CI for these states the contribution ($c^2$) of Rydberg-type configurations amounts to 36% and 27%, respectively. The most striking change is that between the original $2^1A'$ and $3^1A'$ states two additional states appear at 7.6 and 7.7 eV, which have nearly purely Rydberg character. For acrolein Walsh[20] also found Rydberg states in the vicinity of the $2^1A'$ state from vacuum UV absorption spectroscopy. On adding diffuse AOs the energies of the lower excited states, however, do again change less than ±0.25 eV, while the energy of the ground state changes hardly at all. Although we have not checked the influence of diffuse AOs for HD and OT, we expect their importance to decrease with increasing chain length. The larger extension of the π-electron system will add to the resonance energy of the ππ* states, at which point the levels will consequently become lower in energy. The excitation energies of the Rydberg states, on the other hand, are expected to remain constant at a level of about 7–8 eV above the ground state.

In summary, the main limitation of the present calculations concerns the neglect of diffuse AOs, which chiefly results in overlooking Rydberg-type excited states. For the energy levels that are lower than 7.5 eV we estimate the error to be about

(19) Poirier, P.; Kasi, R.; Czismadia, I. G. *Handbook of Gaussian Basis sets, Physical Sciences Data 24*; Elsevier: Amsterdam, 1985.
(20) Walsh, A. D. *Trans. Faraday Soc.* **1945**, *41*, 498.
(21) Hudson, B. S.; Loda, R. T. *Chem. Phys. Lett.* **1981**, *81*, 591.

Table IV. Orbital Energies of the n, $\pi$, and $\pi^*$ Molecular Orbitals for Crotonaldehyde, Hexadienal, and Octatrienal in Both the G and E Geometries

| | energy (hartree) | | |
|---|---|---|---|
| | n(a′) | $\pi_3$(a″) | $\pi_4^*$(a″) |
| CA(G) | −0.4284 | −0.3794 | +0.0801 |
| HD(G) | −0.4252 | −0.3285 | +0.0621 |
| OT(G) | −0.4248 | −0.3029 | +0.0507 |
| CA(E) | −0.4280 | −0.3551 | +0.0405 |
| HD(E) | −0.4124 | −0.3003 | +0.0120 |
| OT(E) | −0.4007 | −0.2667 | −0.0068 |

0.25–0.30 eV from the above considerations and the observed extrapolation uncertainty.

## 4. Discussion

**1. Nature and Energy of Molecular Orbitals.** In order to grasp the nature of the lower excited states that are calculated in the CI procedure (section 3.1) we examine the character of the MOs as retrieved from the SCF calculations. From Tables I–III we observe that the MOs that predominantly participate in the excitations are the highest occupied molecular orbital of a′ symmetry, n, and both the highest occupied and lowest unoccupied molecular orbitals of a″ symmetry, $\pi_3$ and $\pi_4^*$, respectively. We perform a Mulliken population analysis for these MOs to obtain a measure for the distribution of the electron density over the AOs. For CA in the G geometry this analysis shows that for the n-orbital about two-thirds of the electron density is concentrated on the oxygen 2p AO that lies in the plane of the polyenal and perpendicular to the carbonyl bond; the remainder of the electron density is chiefly distributed over the carbonyl proton and the in-plane 2p AOs of the $\alpha$- and $\beta$-carbons. In the E geometry the contribution from the 2p AO on oxygen amounts to even 80%. For both geometries the distribution of the electron density over the AOs does not change from CA to OT: the MO remains predominantly localized on the oxygen lone pair. Neither lengthening the chain nor relaxing the geometry affect the energy of the n-orbital significantly (Table IV). An ab initio treatment with a minimal Slater-type AO basis has shown that for acrolein, $CH_2$=CH—CHO, also the n-orbital is mainly localized on the oxygen lone pair.[22]

Analysis of $\pi_3$, the highest occupied a″-orbital, demonstrates that for this orbital the electron density at the carbonyl carbon is virtually zero for all polyenals and all geometries studied. The orbital is found to be delocalized over the whole chain including the methyl out-of-plane hydrogen atoms. Lengthening of the polyenal results in a redistribution of the electron density along the polyenal. The energy of this $\pi$-orbital is less negative than that of the n-orbital (Table IV), and it significantly increases on lengthening the chain and on bond-order reversal.

The lowest unoccupied orbital of a″ symmetry, $\pi_4^*$, is fairly uniformly distributed along the polyenal for all compounds. The small positive value of the corresponding energy decreases on increasing the chain length and on bond-order reversal (Table IV). For OT the energy of $\pi_4^*$ in the E geometry is even slightly negative. In Figure 4 we schematically represent for CA in the G geometry the three MOs that participate in the lower excited states. From this figure one can qualitatively perceive that upon $\pi\pi^*$ excitation the polyenals tend to bond-order reversal; the $\pi$-orbital is bonding between the two central carbon atoms and nonbonding between the $\alpha$- and $\beta$-carbon, while the $\pi^*$-orbital is antibonding between the two central carbon atoms and bonding between the $\alpha$- and $\beta$-carbon.

**2. Excited Singlet States.** In order to facilitate a comparison of the calculated electronic states with experimental results we have also labeled the former according to the spectroscopic usage (cf. first column of Tables I–III). In doing so we only account for the nature of the MOs that play a role in the dominant configurations. For CA in the G geometry this leads to the following

(22) Devaquet, A. *J. Am. Chem. Soc.* **1972**, *94*, 5160.

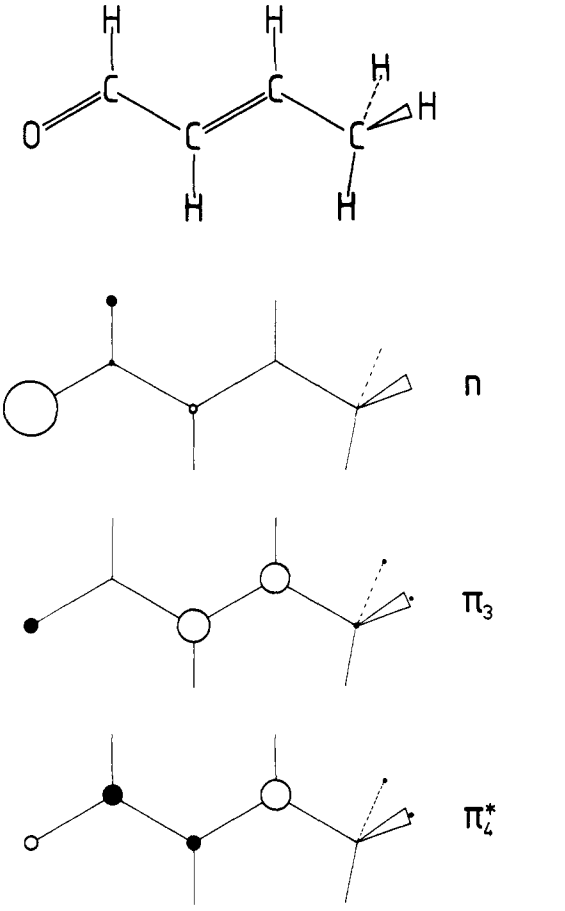


**Figure 4.** Schematic representation of the n, $\pi$, and $\pi^*$ molecular orbitals for crotonaldehyde. The diameter of the circles is proportional to the probability of finding an electron at an atom. Full and open circles refer to positive and negative signs of the coefficients of the dominant AO at an atom.

Table V. Calculated Energy Differences of Some Lower Excited States with Respect to the Ground State in the G Geometry[a]

| state | CA(G) (eV) | CA(E) (eV) | HD(G) (eV) | HD(E) (eV) | OT(G) (eV) | OT(E) (eV) |
|---|---|---|---|---|---|---|
| $S_0$ | 0.00 | 0.38 | 0.00 | 0.62 | 0.00 | 0.80 |
| $^1B_u^*$ | 6.59 | 6.12 | 5.92 | 5.65 | 5.19 | 4.81 |
| $^1A_g^*$ | 8.18 | 6.55 | 6.33 | 4.31 | 5.57 | 3.72 |
| $^1n\pi^*$ | 4.07 | 3.28 | 4.19 | 3.22 | 3.86 | 2.66 |
| $^3\pi\pi^*$ | 3.91 | 2.96 | 3.13 | 2.13 | 2.24 | 1.50 |
| $^3n\pi^*$ | 3.78 | 3.14 | 3.66 | 2.99 | 3.41 | 2.28 |

[a] The states are labeled according to spectroscopic usage.

assignments. The lowest excited singlet state, which is of A″ symmetry, represents a $^1n\pi^*$ state. The $2^1A'$ state, which corresponds to an excitation of one electron from $\pi_3$ to $\pi_4^*$, is the lowest $^1\pi\pi^*$ state. In the case of $C_{2h}$ symmetry, which applies to polyenes, the $2^1A'$ and $3^1A'$ states would be of $B_u$ and $A_g$ character, respectively. Hence they are presently distinguished by the notation $^1B_u^*$ and $^1A_g^*$. In Table V we enumerate for both the G and E geometry the energy differences of some lower excited states with respect to the ground state in the G geometry.

For polyenals with $n$ = 1, 2, and 3 we have determined the $^1n\pi^*$ state to be the lowest excited singlet state. In the G geometry $S_2$ is of $B_u^*$ and $S_3$ of $A_g^*$ character. For polyenals without the terminal methyl group, PPP-SCF-MO-CI calculations resulted in the same state ordering for the $^1n\pi^*$ and $^1B_u^*$ states.[8] At that time the presence of a singlet state of $A_g^*$ nature had not yet been recognized. According to our calculations the $^1n\pi^*$ state hardly undergoes a red shift on lengthening the chain and the $^1A_g^*$ state decreases more in energy than the $^1B_u^*$ state. On extrapolating this calculated trend to longer polyenals we expect the $^1A_g^*$ state to become the lowest excited singlet state. These results fully agree

with the singlet-state ordering for polyenals as a function of chain length derived from singlet–singlet absorption spectra. For polyenals with $n \leq 3$ the lowest excited singlet state is $n\pi^*$ in nature. For decatetraenal ($n = 4$)[2] and dodecapentaenal ($n = 5$)[21] the $^1n\pi^*$, $^1B_u^*$, and $^1A_g^*$ states were reported to be about degenerate, while for longer polyenals the lowest excited singlet state was claimed to be of $A_g^*$ character.[2] The difference in the presently calculated trends for A′ and A″ states on increasing the chain length can be rationalized in view of the energies of the MOs involved in the excitations (see section 4.1). This analysis shows that lengthening of the chain results in no change in the energy of the n-orbital, a substantial change in the energy of the $\pi$-orbital, and a smaller change in the energy of the $\pi^*$-orbital.

We observe a distinct analogy between the lower excited $^1A'$ states of polyenals and the corresponding singlet states of polyenes. Considering the wave functions, we note that for polyenes the $1^1B_u$ state was claimed to be a simple $\pi$ to $\pi^*$ excitation.[9] As for polyenals, a proper account of the $\pi$-electron correlation is especially important for the description of the polyene $2^1A_g$ state. Only by including doubly excited character is this state correctly predicted to be lower in energy than the $1^1B_u$ state.[10] For polyenals though the contribution of the doubly excited configuration seems to be smaller than for polyenes. In the present ab initio calculations for OT in the G geometry the $A_g^*$ state contains 23% doubly excited character (Table III), whereas in PPP-SCF-MO-CI calculations for octatetraene in a similar geometry the $2^1A_g$ state was found to contain 35% doubly excited character.[9] Concerning the state ordering, we have calculated for polyenals the $^1A_g^*$ state to lower more in energy upon lengthening the chain than the $^1B_u^*$ state. The same trend was observed for the $^1A_g$ as compared to the $^1B_u$ state for polyenes.[23] The crossing of those two polyene singlet states, however, already occurs for less than three double bonds[11] instead of, as for the polyenals, for five or six double bonds, which may be related to the larger amount of doubly excited character in the polyene $2^1A_g$ state.

We presently obtain for CA an energy difference between $S_0$ in the G geometry, $S_0(G)$, and $S_1$ in the E geometry, $S_1(E)$, of 3.28 eV (cf. Table V), while the transition energy ascribed to the 0–0 transition in vapor-phase absorption spectra was found to be 3.29 eV.[3] As far as a comparison is meaningful—we have only performed calculations for a few fixed geometries, so we do not know the minimum energies of the excited states—these two values agree surprisingly well with each other. Similarly, the energy of the vertical $S_0(G) \rightarrow S_1(G)$ transition as calculated for CA (4.07 eV) is close to the energy of the band maximum observed in the absorption spectra of CA in perfluoro-*n*-hexane (3.78 eV);[2] this comparison though should also be considered with some caution, since we did not calculate in full the dependence of the transition moment on the nuclear coordinates. According to both our calculations and experiments[2] the energy of the $^1n\pi^*$ state remains about constant upon lengthening the chain and, consequently, the agreement between theory and experiment for HD and OT is similar to that for CA. Concerning the $^1B_u^*$ state, INDOUV calculations for CA (G geometry) led to a vertical excitation energy from the ground state of 6.16 eV[7] as compared to 6.59 eV presently obtained. With regard to the $^1B_u^*$ state of the longer polyenals, HD and OT, only low-resolution absorption spectra have been recorded which hampers an assignment of the observed bands. Consequently, we are only able to compare our calculated excitation energies with a range of experimental values. For HD in perfluoro-*n*-hexane the onset of the absorption was found at about 4.21 eV and the band maximum at about 4.90 eV,[2] while the calculated transition energies are at 5.65 eV ($S_0(G) \rightarrow {}^1B_u^*(E)$) and 5.92 eV ($S_0(G) \rightarrow {}^1B_u^*(G)$). For OT in perfluoro-*n*-hexane the onset of the absorption was found at about 3.72 eV and the band maximum at about 4.32 eV,[2] while the calculated transition energies are at 4.81 eV ($S_0(G) \rightarrow {}^1B_u^*(E)$) and 5.19 eV ($S_0(G) \rightarrow {}^1B_u^*(G)$). Although we have to bear in mind that the comparison between calculated and experimental values has its limits, we note that the values calculated for the $^1B_u^*$ state seem to be systematically too high. As regards the location of the $^1A_g^*$ state for small polyenals ($n = 1, 2, 3$), neither experimental nor theoretical values have been reported so far.

**3. Lowest Triplet States.** As for the excited singlet states, we label the lowest triplet states according to spectroscopic usage; in view of the MOs that play a role in the excitations, the $^3A'$ and $^3A''$ states are denominated $^3\pi\pi^*$ and $^3n\pi^*$, respectively.

The MRD-CI calculations demonstrate that for polyenals with $n = 2$ and 3 the lowest triplet state is of $\pi\pi^*$ character. For polyenals without the terminal methyl group a similar conclusion was drawn from PPP-SCF-MO-CI calculations.[8] Our calculations corroborate the results of recent ESE experiments,[6] from which the lowest triplet state was found to be a $^3\pi\pi^*$ state for polyenals with $n = 2$–5. In addition that study also showed that the zero-field splittings are inversely proportional with $n + 1$. This relationship could be reproduced by solely accounting for spin–spin dipolar interaction while describing $T_0$ in a Hückel approximation as an excitation of one electron from the highest occupied $\pi$-orbital to the lowest unoccupied $\pi^*$-orbital. The success of this model pointed already to the simple nature of $T_0$. The results of the CI procedure prove that the $^3\pi\pi^*$ state can indeed be nearly represented by a single $\pi$ to $\pi^*$ excited configuration. The Hückel model provides a reasonable approximation to the wave function of the lowest triplet state, which is supported by the qualitative similarity between the ab initio MOs and the Hückel MOs. For example, in both treatments the electron density in the $\pi$-orbital at the carbonyl carbon atom is vanishingly small.

A comparison of the MRD-CI triplet excitation energies for $n = 2$ and 3 with experimental values is hampered by the scarcity of such data due to the absence of phosphorescence. For HD no information concerning the triplet energy levels is available. For polyenals with $n = 3$, 4, and 5, Evans performed $S_0 \rightarrow T_0$ absorption spectra in the presence of high-pressure oxygen[5] and observed a substantial decrease of the $T_0$ energy level on increasing chain length. Our CI calculations point to a similar trend in the energy of the $^3\pi\pi^*$ state for $n = 1$, 2, and 3. For OT Evans claimed the 0–0 band of the $S_0 \rightarrow T_0$ transition to be at 1.89 eV (15210 $cm^{-1}$) as compared to 1.50 eV, the energy we calculate for the $S_0(G) \rightarrow T_0(E)$ transition.

For CA ($n = 1$) we have found that in the G geometry the $^3n\pi^*$ state is just 0.13 eV lower in energy than the $^3\pi\pi^*$ state. For this compound a similar triplet-state ordering was determined by Boerth from INDOUV calculations.[7] However, his treatment led to smaller excitation energies (2.14 and 3.09 eV) than presently obtained (3.78 and 3.93 eV) and to a much larger energy difference between the two triplet states (0.95 eV as compared to 0.13 eV). For the E geometry of CA we have calculated a reversed triplet-state ordering. Apparently, bond-order reversal stabilizes the $^3\pi\pi^*$ state more than the $^3n\pi^*$ state, as opposed to the result obtained by ab initio calculations for acrolein.[22]

Explicit experimental data concerning the triplet of CA were given by Birge et al.,[3] who reported the lowest triplet state to be of $n\pi^*$ character. The band in the room temperature $S_0 \rightarrow T_0$ absorption spectra that they assigned to the 0–0 transition was found at 3.09 eV. With the same reserve as for the singlet states we may compare this value to 3.14 eV, the energy we calculate for the $S_0(G) \rightarrow {}^3n\pi^*(E)$ transition. They found a $^1n\pi^*$–$^3n\pi^*$ energy gap of 0.195 eV, close to the $^1n\pi^*(E)$–$^3n\pi^*(E)$ energy gap presently obtained (0.14 eV). Yamauchi et al.[4] performed time-resolved EPR experiments on the lowest triplet state of CA, from which they argued this state to be $\pi\pi^*$ in nature. This assignment is in accordance with our calculations. They explained the small zero-field splittings of CA as compared to those of rigid conjugated enones as being caused by a twist about the C=C bond, a twist that was predicted to stabilize the $^3\pi\pi^*$ state for acrolein.[22] In our treatment we have not allowed for such an out-of-plane distortion. The small triplet–triplet energy gap for CA may give rise though to geometry changes induced by vibronic coupling between the participating $^3A'$ and $^3A''$ states through an out-of-plane vibrational mode. The near degeneracy of the $^3n\pi^*$ and $^3\pi\pi^*$ states as obtained from the calculations is consistent with the observation that the triplet-state ordering for $\alpha,\beta$-un-

(23) Kohler, B. E. *J. Chem. Phys.* **1988**, *88*, 2788.

Table VI. The Absolute Values of the Spin–Orbit-Coupling Matrix Elements, the $x$ Component of the Transition Moments Corresponding to the $^1n\pi^* \rightarrow S_0$ and $^3n\pi^* \rightarrow {}^3\pi\pi^*$ Transitions ($x$ Corresponds to the Direction Perpendicular to the Molecular Plane), the Oscillator Strength of the $^3\pi\pi^* \rightarrow S_0$ Transition ($f = {}^2/_3\Delta E\mu^2$, with $\Delta E$ in hartree and $\mu$ in au), and the Phosphorescence Lifetime of the $T_z$ Sublevel of the $^3\pi\pi^*$ State for Crotonaldehyde, Hexadienal, and Octatrienal in Both the G and E Geometries

| | $\langle n\|\mathcal{H}_{soc}\|\pi_3\rangle$ ($cm^{-1}$) | $\langle\pi_4^*\|\mathcal{H}_{soc}\|n\rangle$ ($cm^{-1}$) | $\mu_x(^1n\pi^*,S_0)$ (au) | $\mu_x(^3n\pi^*,{}^3\pi\pi^*)$ (au) | $f(^3\pi\pi^*,S_0)$ | $\tau$ (s) |
|---|---|---|---|---|---|---|
| CA(G) | 31.1 | 40.8 | $2.7 \times 10^{-2}$ | $1.7 \times 10^{-2}$ | $4.3 \times 10^{-8}$ | $3.5 \times 10^{-2}$ |
| HD(G) | 22.8 | 36.0 | $1.8 \times 10^{-2}$ | $1.2 \times 10^{-2}$ | $3.0 \times 10^{-10}$ | 8.2 |
| OT(G) | 18.1 | 31.5 | $1.6 \times 10^{-2}$ | $1.0 \times 10^{-2}$ | $6.2 \times 10^{-11}$ | $7.5 \times 10^{1}$ |
| CA(E) | 47.9 | 42.5 | $1.2 \times 10^{-2}$ | $4.3 \times 10^{-3}$ | $3.4 \times 10^{-9}$ | 1.0 |
| HD(E) | 40.0 | 34.8 | $1.4 \times 10^{-2}$ | $3.3 \times 10^{-3}$ | $1.9 \times 10^{-10}$ | $5.4 \times 10^{1}$ |
| OT(E) | 35.7 | 28.7 | $5.3 \times 10^{-3}$ | $2.6 \times 10^{-3}$ | $1.1 \times 10^{-11}$ | $4.4 \times 10^{3}$ |

saturated carbonyl compounds subtly depends on the environmental conditions and on the substituents at the enone chromophore.[24]

**4. Decay of the Lowest Triplet State.** The lowest $\pi\pi^*$ triplet state of polyenals with $n = 2$–5 was previously found to decay within tens of microseconds in a nonradiative way.[6] In order to gain insight into the origin of the absence of phosphorescence we estimate the radiative lifetime of the lowest $\pi\pi^*$ triplet state for the polyenals under study. Although we have found for CA (G geometry) $T_0$ to be of $n\pi^*$ character, we consider the radiative lifetime for the $^3\pi\pi^*$ state in order to enable a comparison with the observed phosphorescence lifetimes of the $\pi\pi^*$ triplet states of conjugated enones.

We regard CA, HD, and OT in both the G and the E geometries and calculate $f(^3\pi\pi^*, S_0)$, the oscillator strength of the $^3\pi\pi^* \rightarrow S_0$ transition, and from that the radiative lifetime of the $^3\pi\pi^*$ state. In the first approximation the $^3\pi\pi^* \rightarrow S_0$ transition is spin-forbidden and $f(^3\pi\pi^*, S_0)$ is zero. A finite radiative lifetime results from spin–orbit coupling which may introduce singlet character into $^3\pi\pi^*$ and triplet character into $S_0$. The transition moment for the $^3\pi\pi^* \rightarrow S_0$ transition becomes (apart from a small normalization factor)

$$\begin{aligned}\vec{\mu} &= \langle \Psi_{^3\pi\pi^*} + \lambda_1\Psi_{^1n\pi^*}|\vec{\mu}|\Psi_{S_0} + \lambda_2\Psi_{^3n\pi^*}\rangle \\ &= \lambda_1\langle\Psi_{^1n\pi^*}|\vec{\mu}|\Psi_{S_0}\rangle + \lambda_2\langle\Psi_{^3\pi\pi^*}|\vec{\mu}|\Psi_{^3n\pi^*}\rangle \end{aligned} \quad (1)$$

with

$$\lambda_1 = \langle\Psi_{^1n\pi^*}|\mathcal{H}_{soc}|\Psi_{^3\pi\pi^*}\rangle/[E(^3\pi\pi^*) - E(^1n\pi^*)]$$

$$\lambda_2 = \langle\Psi_{^3n\pi^*}|\mathcal{H}_{soc}|\Psi_{S_0}\rangle/[E(S_0) - E(^3n\pi^*)]$$

In writing this expression for $\vec{\mu}$ we have realized that in our approximation the spin–orbit-coupling matrix elements of $^3\pi\pi^*$ with $^1B_u^*$, $^1A_g^*$, and $S_0$ tend to zero. In addition, we have only taken into account the excited states considered in Table V and neglected higher lying ones because the contribution to the oscillator strength strongly decreases with increasing energy gap. We calculate the spin–orbit-coupling matrix elements not on the CI but on the SCF level and represent the $^3\pi\pi^*$ state by a single configuration corresponding to the excitation from $\pi_3$ to $\pi_4^*$ and the $^3n\pi^*$ and $^1n\pi^*$ states by a single configuration corresponding to the excitation from n to $\pi_4^*$. The remaining spin–orbit-coupling matrix elements are $\langle n|\mathcal{H}_{soc}|\pi_3\rangle$ and $\langle\pi_4^*|\mathcal{H}_{soc}|n\rangle$. We used the following expression for $\mathcal{H}_{soc}$

$$\mathcal{H}_{soc} = \frac{e^2\hbar}{8\pi\epsilon_0 m^2c^2}\sum_{i,\alpha}\frac{Z_{eff}^{\alpha}}{r_{i\alpha}^3}(\vec{r}_{i\alpha} \times \vec{p}_i)\cdot\vec{S}_i$$

where $\alpha$ refers to nuclei, $i$ refers to electrons with position $\vec{r}_{i\alpha}$ and momentum $\vec{p}_i$, and $\vec{S}_i$ is the spin operator. The two-electron (spin-other-orbit) interaction is accounted for by taking effective nuclear charges $Z_{eff}^{\alpha}$. We used the values given by Clementi:[25] $Z_{eff}^{O} = 4.4532$, $Z_{eff}^{C} = 3.1358$, and $Z_{eff}^{H} = 1$. We expand the matrix elements $\langle n|\mathcal{H}_{soc}|\pi_3\rangle$ and $\langle\pi_4^*|\mathcal{H}_{soc}|n\rangle$ over AOs. In doing so we neglect two-center terms, since according to Cooper[26] these are approximately an order of magnitude smaller than the one-center terms. The remaining one-center one-electron matrix elements are calculated[27] with the employed AO basis set. The matrix elements of the $z$ component of $(\vec{r}_{i\alpha} \times \vec{p}_i)$ are at least an order of magnitude larger than the corresponding ones for the $y$ component ($z$ and $y$ refer to inplane axes parallel and perpendicular to the carbonyl bond, respectively). Consequently, the dominant contribution to the radiative decay is expected to come from the spin sublevel $T_z$ and we can consider the triplet state as a one-level system.[28] The natural radiative lifetime $\tau$ of the $T_z$ sublevel of the $^3\pi\pi^*$ state then is given by

$$\tau = \frac{1.5}{f(^3\pi\pi^*,S_0)[E(^3\pi\pi^*) - E(S_0)]^2} \quad (2)$$

with the energy gap in $cm^{-1}$ and $\tau$ in seconds. In employing eqs 1 and 2 we take the energy gaps from Tables I–III and compute the matrix elements of $\mu_x$ on the CI level. In Table VI we enumerate the magnitude of the spin–orbit-coupling matrix elements, the transition moments, the oscillator strength $f(^3\pi\pi^*,S_0)$ and the radiative lifetime $\tau$.

For $n = 1$ in the G geometry this lifetime, 35 ms, approaches the experimentally observed phosphorescence lifetime of the $^3\pi\pi^*$ state of rigid conjugated enones at 1.4 K (20 to 60 ms).[29] The radiative lifetime becomes substantially longer upon lengthening the chain and upon relaxing the polyenals to the E geometry (Table VI). From ESE experiments we found for polyenals ($n = 2$–5) at 1.2 K the triplet lifetime to be in the order of tens of $\mu$s and to decrease systematically with increasing chain length.[6] By comparing for OT the calculated radiative lifetime and the observed radiationless lifetime (77 $\mu$s) we estimate the quantum yield of phosphorescence for the $T_z$ sublevel to be only $10^{-6}$ (G geometry) or $1.8 \times 10^{-8}$ (E geometry). Extrapolating to longer polyenals we expect this quantum yield to decrease even more. In summary, the calculated radiative triplet lifetimes substantiate the essentially nonradiative decay of the lowest triplet state for longer polyenals. The absence of phosphorescence for these polyenals is due to the fast radiationless decay in combination with an extremely long radiative lifetime.

## 5. Conclusion

We have established the nature of the lower excited states of three short-chain polyenals by means of MRD-CI calculations. The dependence of the singlet- and triplet-state ordering on chain length and geometry as predicted by the calculations is consistent with experimental observations. For crotonaldehyde, hexadienal, and octatrienal we have determined the lowest excited singlet state to be of $n\pi^*$ character. For polyenals larger than crotonaldehyde

(24) Marsh, G.; Kearns, D. R.; Schaffner, K. *J. Am. Chem. Soc.* **1971**, *93*, 3129. Jones, C. R.; Kearns, D. R. *J. Am. Chem. Soc.* **1977**, *99*, 344. Blok, P. M. L.; Jacobs, H. J. C.; Dekkers, H. P. J. M. *J. Am. Chem. Soc.* **1991**, *113*, 794.

(25) Clementi, E. Tables of Atomic Functions; *IBM J. Res. Dev. Suppl.* *9* **1965**, 2.

(26) Richards, W. G.; Trivedi, H. P.; Cooper, D. L. *Spin–orbit coupling in molecules*; Claredon Press: Oxford, 1981.

(27) Chandra, P.; Buenker, R. J. *J. Chem. Phys.* **1983**, *79*, 358.

(28) The in-plane principal axes of the fine-structure tensor need not be parallel to $y$ and $z$. For the polyenals with $n = 3$, 4, and 5 these principal axes have been found to be rotated by 10°, 12°, and 14° with respect to the direction of the carbonyl bond.[6] In order not to complicate the present analysis further we have omitted this slight rotation here because it does not influence our conclusions.

(29) Jones, C. R.; Maki, A. H.; Kearns, D. R. *J. Chem. Phys.* **1973**, *59*, 873.

$T_0$ is a $^3\pi\pi^*$ state. In the wave function of this state $\pi$-electron correlation hardly plays a role; $T_0$ is well represented by a single configuration that corresponds to an excitation of a single electron from the highest occupied $\pi$ to the lowest unoccupied $\pi^*$ molecular orbital. In view of such a simple description of $T_0$ it would be worthwhile to try and calculate from the present ab initio wave function the zero-field splittings of $T_0$ and the spin-density distribution along the polyenal chain. Finally, for octatrienal we have found a large difference between the calculated radiative lifetime of the $T_z$ sublevel of $T_0$ and the experimentally observed radiationless lifetime. This discrepancy even increases on lengthening the chain and explains the total absence of polyenal phosphorescence.

**Acknowledgment.** The Theoretical Chemistry group of the University of Bonn is acknowledged for making available the MRD-CI computer program. We thank J. H. van der Waals for stimulating discussions concerning the treatment of the spin-orbit coupling and Aafke Stehouwer for her contributions to the calculations. This work was supported by The Netherlands Foundation for Chemical Research (SON) with financial aid from The Netherlands Organization for Scientific Research (NWO).

# Theoretical Study on Mechanism and Selectivity of Electrophilic Aromatic Nitration

**Kálmán J. Szabó,* Anna-Britta Hörnfeldt, and Salo Gronowitz**

*Contribution from the Division of Organic Chemistry 1, Chemical Center, University of Lund, P. O. Box 124, S-221 00 Lund, Sweden.* *Received January 6, 1992*

**Abstract:** Reaction profiles for the aromatic nitration reaction have been calculated. Stationary points were located and characterized at the ab initio HF/3-21G level. Single point MP4DQ/3-21G calculations were carried out to evaluate the correlation energy correction for the activation barrier heights. Unsolvated nitronium ion reacts with benzene to give the Wheland intermediate without an energy barrier. Solvated nitronium ion (protonated methyl nitrate) reacts with aromatics to give an activation barrier which is substituent dependent, but also depends on the solvating species. The positional selectivity is produced after this barrier and is independent of the matrix effects. Some predictions were made with regard to the condensed phase nitration reaction.

Aromatic nitration is of outstanding importance in the theory of organic reactivity. In spite of the huge body of accumulated data, the mechanism of aromatic nitration continues to be the subject of active research and some controversy.[1,6] An interesting feature is, for example, that the rate of nitration of toluene relative to benzene depends strongly on the solvent and reagent, while the ratio of ortho-, meta-, and para-substituted products only slightly varies (Table I).

The theoretical investigation of aromatic nitration is complicated by the fact that most of the findings refer to condensed-phase experimental conditions, and the role of solvent effects is not clear. Examining the gas-phase reaction of protonated alkyl nitrates with aromatics, Cacace and Attinâ[4,5,7] pointed out the fundamental similarity between gas-phase and liquid-phase nitration. These gas-phase studies opened new perspectives for the theoretical investigation of mechanistic details of the aromatic nitration.

## Computational Aspects

The Gaussian 86 and Gaussian 90 computer programs[8] were used on a Cray X/MP-416 supercomputer. Restricted Hartree-Fock (RHF) calculations and fourth-order Møller-Plesset correlation energy calculations for double and quadruple substitutions (MP4DQ) were performed using the split valence 3-21G basis set. Stationary structures and points of reaction profiles were optimized by using Schlegel's gradient technique.[9] The final optimization of the stationary points was carried out with no restrictions on internal coordinates. The optimization of the possible Wheland intermediates (WI) and transition states (TS) of benzene nitration continued until the largest remaining force was less than 0.0001 au. The reason for this rather tight convergence criterion is our interest in the structure of these species. The optimization of TS structures is complicated by the flat potentials of geometry parameters describing the conformation of reagent relative to the ring system. The very slow convergence of the geometry optimization of $\pi$-complexes is due to the same problem. Therefore, their geometries were optimized until the forces dropped below 0.002 au, but it was ensured that their total energy did not change more than 0.05 kJ/mol in the last five geometry-optimization steps. At the highest level of theory, MP4DQ/3-21G single point calculations were performed on the HF/3-21G geometries of stationary points obtained along the benzene nitration pathways.

## Results and Discussion

**Reaction of Benzene with Nitronium Ion.** The energy profile for the reaction between benzene and the nitronium ion was calculated (Table II, Figure 1). The distance between the nitrogen atom of the nitronium ion and the attacked carbon atom was chosen as the reaction coordinate (RC). Points of the reaction profile were obtained by freezing the reaction coordinate and optimizing the rest of the internal coordinates simultaneously. No activation barrier was found along the chosen reaction coordinate. The experimental results led to the same conclusions: the gas-phase reaction of benzene with nitronium ion is very exothermic, and vitually no energy barrier is involved.[10] At large RC values

(1) Olah, G. A. *Nitration Methods and Mechanisms*; VCH: New York, 1989; pp 117-218.
(2) Masci, B. *Tetrahedron* **1989**, *45*, 2719.
(3) Masci, B. *J. Chem. Soc., Chem. Commun.* **1982**, 1262.
(4) Attinâ, M.; Cacace, F. *Gazz. Chim. Ital.* **1988**, *118*, 241 and references therein.
(5) Attinâ, M.; Cacace, F.; Ricci, A. *Tetrahedron* **1988**, *44*, 2015.
(6) Schofield, K. *Aromatic Nitration*; Cambridge University Press: Cambridge, 1980; pp 44-54, 104-128.
(7) Attinâ, M.; Cacace, F.; Yañez, M. *J. Am. Chem. Soc.* **1987**, *109*, 5092.
(8) Frisch, M. J.; Head-Gordon, M.; Trucks, G. W.; Foresman, J. B.; Schlegel, H. B.; Raghavachari, K.; Robb, M. A.; Gonzales, C.; Whiteside, R. A.; Seeger, R.; Melius, C. F.; Baker, J.; Binkley, J. S.; DeFrees, D. J.; Fox, D. J.; Martin, R. L.; Khan, L. R.; Stewart, J. J. P.; Topiol, S.; Flender, E. M.; Pople, J. A. *Gaussian 86* and *Gaussian 90*, Gaussian, Inc.: Pittsburgh, PA, 1986 and 1990.
(9) Schlegel, H. P. *J. Comput. Chem.* **1982**, *3*, 214.
(10) Morrison, J. D.; Stanney, K.; Tedder, J. M. *J. Chem. Soc., Perkin Trans. 2* **1981**, 967.

0002-7863/92/1514-6827$03.00/0 